Supporting Information

Manipulating the structural and electronic properties of epitaxial $SrCoO_{2.5}$ thin films by tuning the epitaxial strain

Jiali Zhao,[†,‡,§] *HaizhongGuo,*[†,#,*] *Xu He,*[†] *Qinghua Zhang,*[†,§] *Lin Gu,*[†,§] *Xiaolong Li,*[⊥] *Kui-juan Jin,*[†,§,*] *Tieying Yang,*[⊥] *Chen Ge,*[†] *Yi Luo,*[#] *Meng He,*[†] *Youwen Long,*[†,§] *Jia-ou Wang,*[‡] *Haijie Qian,*[‡] *Can Wang,*[†] *Huibin Lu,*[†] *Guozhen Yang,*[†,§]*, and Kurash Ibrahim*[‡,*]

[†]Institute of Physics, Chinese Academy of Sciences, Beijing 100190, China
[‡]Beijing Synchrotron Radiation Facility Institute of High Energy Physics, Chinese Academy of Sciences, Beijing 100049, China
[#]School of Physical Engineering, Zhengzhou University, Zhengzhou, Henan 450001, China
[⊥]Shanghai Synchrotron Radiation Facility (SSRF), Shanghai Institute of Applied Physics, Chinese Academy of Sciences, Shanghai 201204, China
[§]University of Chinese Academy of Sciences, Beijing 100049, China

Email: hguo@zzu.edu.cn

Email:kjjin@iphy.ac.cn

Email: kurash@ihep.ac.cn

Temperature dependences of magnetization of the SCO2.5 films were performed using a superconducting quantum interference device (SQUID, Quantum Design Inc.). Figure 1S exhibits the magnetization of the187-nm-thick SCO2.5 film as a function of temperature and magnetic field, measured at field-cooled mode in a magnetic field of 1000 Oe. It can be seen from Figure 1S that the187-nm-thick SCO2.5 film exhibits antiferromagnetic properties within the measuring temperature regime. The other SCO2.5 thin films with different thicknesses also show the antiferromagnetic properties.

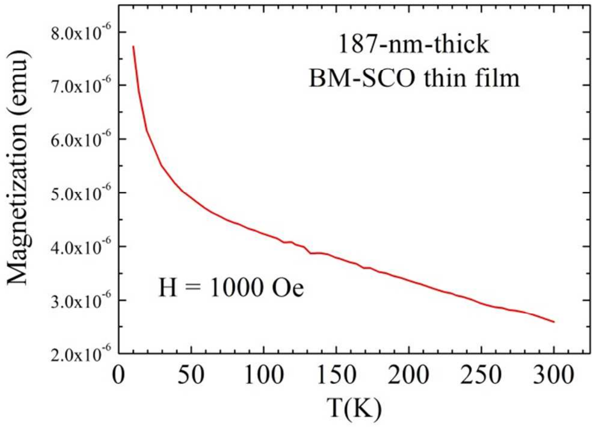

Figure S1. Magnetization as a function of temperature for the 187-nm-thick SCO2.5 thin film measured at field-cooled mode in a magnetic field of 1000 Oe.

Temperature dependences of the resistivityof the SCO2.5 films were performed using a Physical Properties Measurement System (PPMS, Quantum Design Inc.). The standard four-point probe method was used to measure the film resistivity versus temperature (*ρ(T)*). Figure S2 shows the temperature dependences the resistivity of the SCO2.5 thin films the thicknesses of 16, 32, and 180 nm. All these three SCO2.5 thin films are good insulators and show the semiconducting behaviors with temperature. With decreasing the thickness, the resistivity of the SCO2.5 thin film decreases, and the exact reason behind such phenomena maybe be attributed to the change of the content of the oxygen vacancies with the strain.

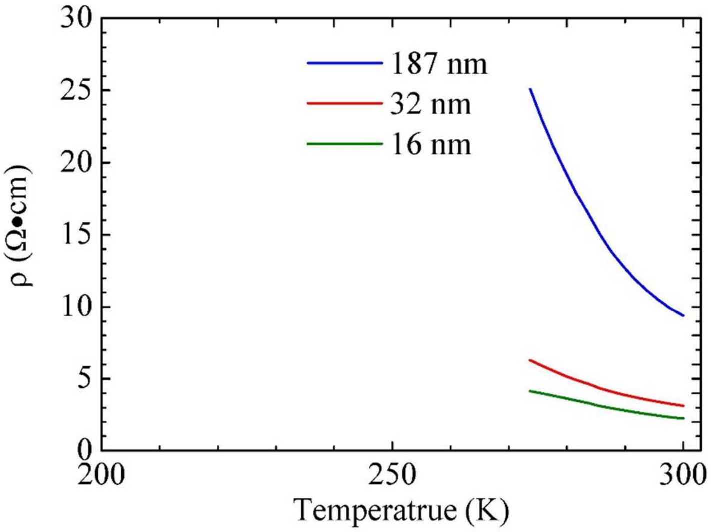

Figure S2. Resistivity versus temperature for the SCO2.5 thin films with the thicknesses of 16, 32, and 187 nm.

To characterize the quality of films, XRD and RSM of the SrCoO2.5 thin films were measured. Figure S3 shows XRD θ-2θ scan pattern of a 32-nm-thick BM-SCO film on the LAO substrate. From Figure S3 it can be seen that expect for (004) and (008) peaks close to the LAO substrate (♦ symbols), there are (002), (006) and (0010) peaks which represent the altering CoO_6 octahedral and CoO_4 tetrahedral layers of the BM phase. Figure S3 indicates that the SCO2.5 thin film deposited on the LAO substrate is at single BM phase. Figure S4 exhibit the XRD θ-2θ patterns ofthe BM-SCO2.5 filmson (001) LAO substrates with different thicknesses of 8, 11, 16, 24, 32, 63, 94, and 187nm, respectively.

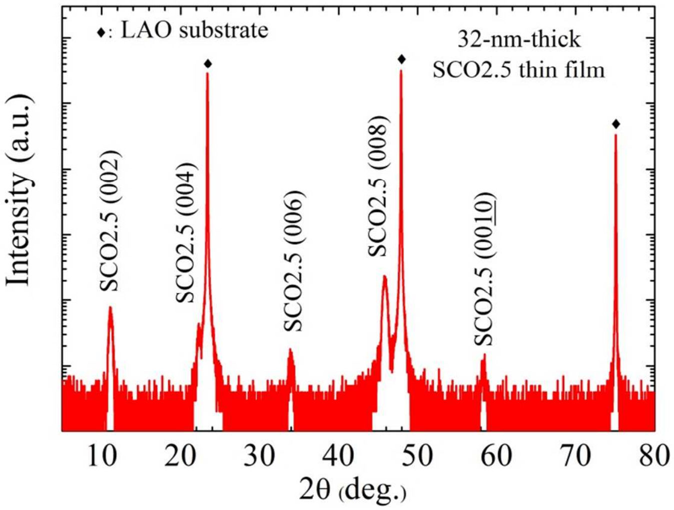

Figure S3. XRD θ-2θ patterns of c-axis-oriented BM-SCO2.5 films epitaxially grown on (001) LAO substrate.

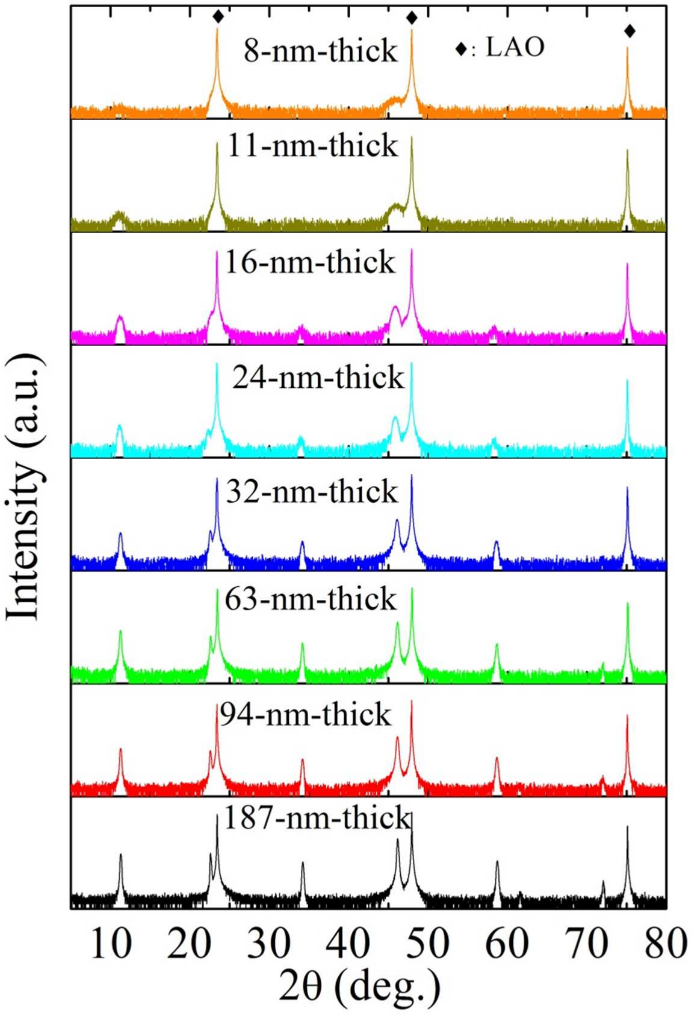

Figure S4. XRD θ-2θ patterns ofthe BM-SCO2.5 filmson (001) LAO substrates with different thicknesses of 8, 11, 16, 24, 32, 63, 94, and 187nm, respectively.

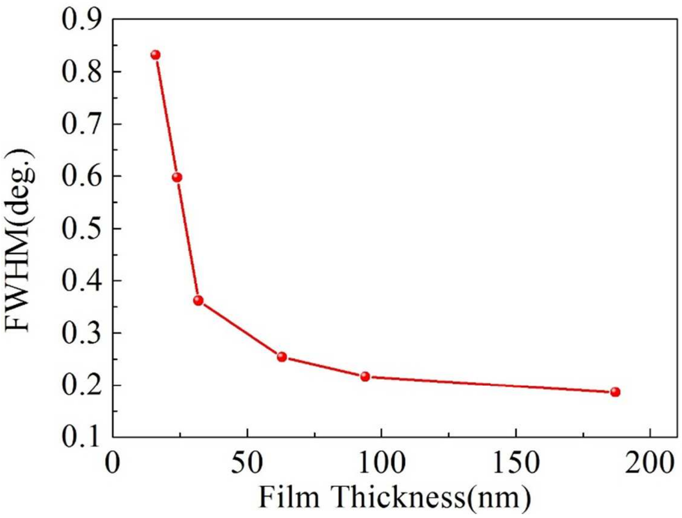

Figure S5.The variation of FWHM of (008) peak with the film thicknesses.

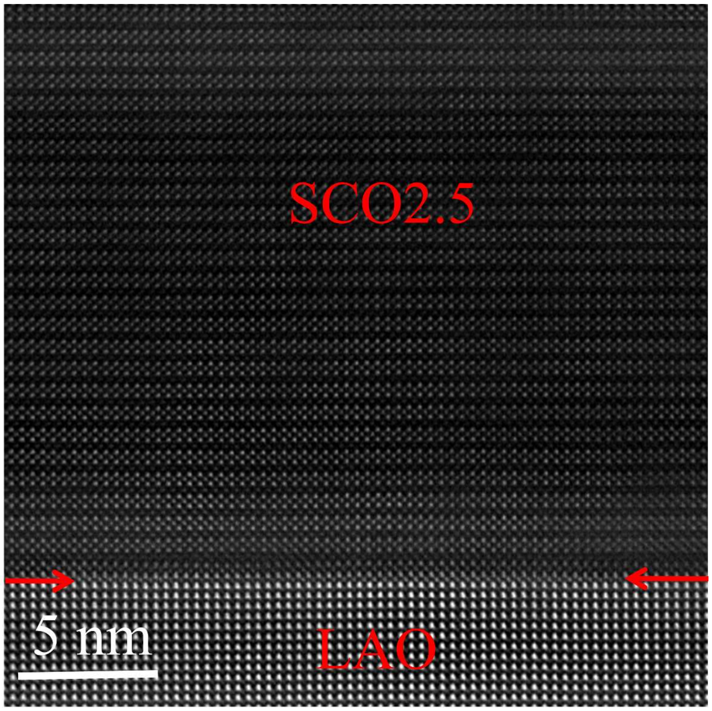

Figure S6.STEM image of 187-nm-thick SCO2.5 film.

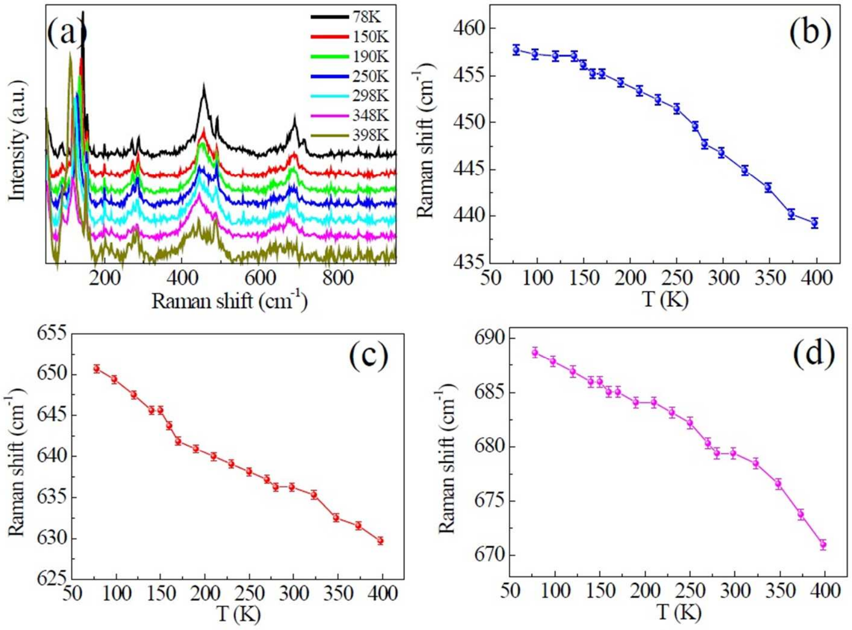

Figure S7.(a) Raman spectra of the 32-nm-thick SCO2.5 thin film measured at different temperature from 78 to 398 K.(b), (c), and (d) Temperature-dependent Raman peak positions of 450, 650, 690 cm^{-1} modes, respectively.

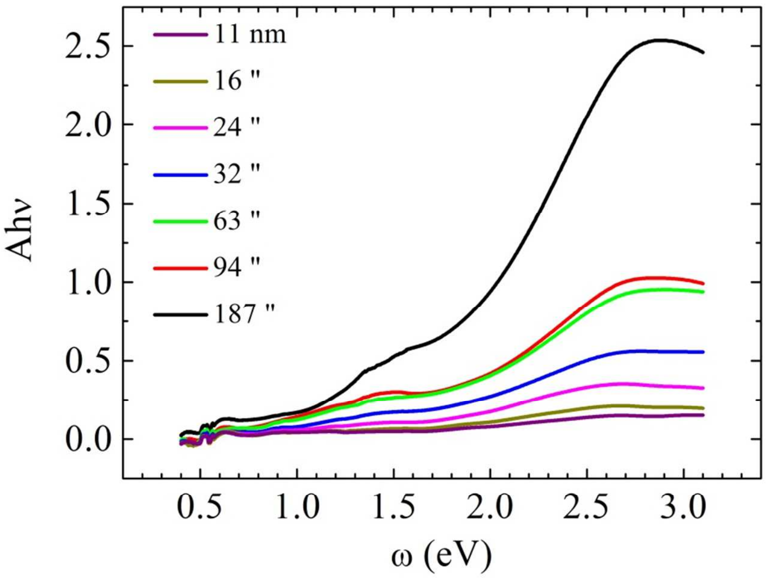

Figure S8. (a) Optical absorption spectra obtained from transmittance measurements of the SrCoO2.5 thin films with different thicknesses.

A comparison of the functionals which are mostly used (LDA, PBE, and PBEsol) and various U values was performed. We noted that indeed the PBEsol +U, where U = 3.5 eV is not optimal. Now we use PBEsol +U, and U = 7.5 eV and redo all the DFT calculations in the manuscript. We also found that the change of the band gap (Fig. 5(c) in the manuscript) was because the calculation converged to a sub-stable state. The change of band gap due to the bi-axial strain is insignificant. Therefore, the DFT result shows that the change of band gap might be due to the structural phase transition or chemical stoichiometry. (We noted that the value of x in $SrCoO_x$ is modulated by the strain, which was reported in Ref. (1). $SrCoO_3$ is a ferromagnetic metal with Co in intermediate spin state whereas SrCoO2.5 is antiferromagnetic with Co in high spin state.)

To find the optimal functional and U value, we tested three functionals: LDA, PBE, and PBEsol and various *U* values from 3 to 7.5 eV, and the results are shown in Table S1. All the parameters give similar electronic structure, both Co1(Co-octahedra) and Co2(Co-tetrahedra) are in the high spin state and have the nominal charge of +3.

LDA gives significantly smaller lattice constants than the experiments. Both PBE and PBEsol lattice constants has less than 2 % deviation from the experimental values. However, PBE gives unreasonably large *c*-axis lattice parameter when the compressive biaxial strain is applied. Therefore, we choose PBEsol, which is optimized for solids. The smaller U (U = 3.5 eV here) gives close *a* and*b* values, which does not reflect the experimental results, therefore, a larger U = 7.5 eV is used, which was also used in Ref. 42. We noted that the chemical stoichiometry can easily deviate from $SrCoO_{2.5}$, therefore, it is better to use a U value which can predict the properties of $SrCoO_3$ as well. A U value of less than 6 eV cannot give the experimentally observed intermediate spin Co state (Ref (2)). Therefore, U = 7.5 eV is suitable for both $SrCoO_{2.5}$ and $SrCoO_3$.

TableS1. A comparison of the functionals (LDA, PBE, and PBEsol) and various U values.

	LDA+U7.5	PBE+U7.5	PBEsol+U3.5	PBEsol+U7.5	Experimental(3)
a (Å)	5.312	5.451	5.478	5.368	5.458
b (Å)	5.475	5.627	5.477	5.534	5.562
c (Å)	15.232	15.699	15.483	15.463	15.637
E_g(eV)	1.64	1.46	0.82	1.75	
m (Co1) (μ_B)	3.2	3.2	2.9	3.2	3.12
m (Co2) (μ_B)	3.1	3.2	2.8	3.2	2.88

TableS2. The relationship of the lattice constants and band gaps.

a (Å)	3.79	3.80	3.81	3.82	3.83	3.84	3.86	3.88	3.90
c (Å)	4.07	4.06	4.05	4.037	4.024	3.883	3.843	3.843	3.82
E_g(eV)	1.50	1.53	1.52	1.52	1.52	1.81	1.84	1.83	1.83

References:

(1). Mitra, C.; Meyer, T.; Lee, H. N.; Reboredo, F. A. Oxygen diffusion pathways in brownmillerite $SrCoO_{2.5}$: Influence of structure and chemical potential. *J. Chem.*

*Phys.***2014**, 141, 084710.

(2).Riveroa, P.; Cazorla, C. Revisiting the zero-temperature phase diagram of stoichiometric $SrCoO_3$ with first-principles methods. *Phys. Chem. Chem. Phys.***2016**, *18*, 30686-30695.

(3). Munoz, A.; Calle, C.; Alonso, J. A.; Botta, P. M.; Pardo, V.; Baldomir, D.; Rivas, J. Crystallographic and magnetic structure of $SrCoO_{2.5}$ brownmillerite: Neutron study coupled with band-structure calculations.*Phys Rev B***2008**, *78*, 054404.